Entropy Displacement and Information Distance Analysis of Electron Distributions in Molecules and Their Hirshfeld Atoms

Roman F. Nalewajski* and Elżbieta Broniatowska

Faculty of Chemistry, Jagiellonian University, R. Ingardena 3, 30-060 Cracow, Poland

Received: February 12, 2003; In Final Form: May 2, 2003

The displacements of the Shannon entropy and its density, relative to the corresponding reference values for the overlapping densities of the free atoms of the isoelectronic "promolecule", are investigated for selected small molecules and propellane systems. A similar analysis is carried out for the Hirshfeld constituent atoms. The entropy difference maps are shown to be qualitatively similar to the corresponding plots of the density difference function and the entropy deficiency density, with respect to the same reference distributions. A use of these quantities as complementary tools for monitoring changes in electronic structure due to the bond formation is advocated. The entropy displacement plots for small-ring propellanes are used to examine the nature of the central bond between the bridgehead carbons. These results are compared with predictions of the previous bond multiplicity study. The [1.1.1]- and [2.1.1]propellanes are found to exhibit a partial "through-bridge" bond and lowering of the electron density and the entropy/entropy deficiency densities between the bridgehead atoms. Larger bridges in the [2.2.1]- and [2.2.2]propellanes generate an increase of the electron and information densities in the central bond region, thus introducing a partial "through-space" bond component.

1. Introduction

The contour maps of several local functions of the molecular electron distributions have been used in the past to probe changes in the electronic structure accompanying the formation of chemical bonds, relative to a collection of the nonbonded constituent atoms of the isoelectronic "promolecule", in which the "frozen" densities of the free atoms are shifted to their actual positions in the molecular system under consideration. For example, the displacements in the electron distribution are directly displayed in plots of the familiar *density difference function*, which were recently shown[1] to be related to the corresponding diagrams of the *information distance density* of the Kullback−Leibler functional[2] of the information theory[2,3] for the *entropy deficiency* (missing information, cross entropy) between the molecular and promolecular distributions of electrons. This analysis has attributed an entropy/information content to the traditional density difference maps. It has also validated the use of the information distance density diagrams[1] and the related *surprisal* plots[1,4] in an information-theoretic analysis of the origins of the chemical bond.

In the present analysis we extend the previous information distance treatment by examining corresponding displacements in the global and local Shannon entropy quantities, relative to the promolecule values, and by comparing these changes with the related density difference and information distance data. The change in the integral entropy of the electron probability distribution reflects a net effect of opposing trends due to electron delocalization and charge transfer, the bonded atom rehybridization and promotion in a molecule, the contraction of atomic densities in the effective field of bonding partners, etc. For example, the covalent bond component, electron promotion to the outer (virtual) atomic orbitals of free atoms, and an electron inflow to an atom in a molecule (AIM), which tend to make the molecular electron distribution more homogeneous and atomic distributions more diffuse, increase the entropy (decrease the order) in the molecule compared to the isoelectronic promolecule. The bonded atom contraction and an electron outflow from a given AIM act in the opposite way, thus decreasing entropy (increasing order) in a molecule. The maps of local entropy displacements carry the information about local contributions to these global entropy shifts, thus identifying the regions of an extra increase or decrease in uncertainty of molecular probability distributions relative to their promolecular references. It is of interest to examine the physical message conveyed by these quantities and to compare it with that transpiring from the associated density difference and entropy deficiency data, which have been examined in previous works.

Chemical interpretations of molecular electron densities, in terms of AIM and bonds that connect them, require an atomic discretization of molecular distributions. The "stockholder" partition of Hirshfeld[5] determines the exponentially decaying, overlapping bonded atoms, which were shown to have a solid basis in the information theory[1,4,6−9] and exhibit several properties that make them attractive concepts for the purpose of extracting a chemical understanding of the experimental or theoretical electron distributions in molecules. In the present study we will apply this division scheme to probe changes in the AIM electronic structure, relative to that of the corresponding free atom, using the contour maps of the density difference function and those for the densities of the atomic entropy displacement and/or entropy deficiency.

2. Hirshfeld Atoms and Entropy Displacements

2.1. Stockholder Division of the Molecular Electron Density. It has been shown by Hirshfeld[5] that a given molecular electron density ρ is exhaustively partitioned into the so-called "stockholder" densities $\{\rho_X^{\mathrm{H}}\} \equiv \boldsymbol{\rho}^{\mathrm{H}}$ of bonded molecular fragments $X = \mathrm{A}, \mathrm{B}, \ldots$, e.g., bonded atoms (Atoms-in-

* To whom correspondence should be addressed. E-mail: nalewajs@chemia.uj.edu.pl.

10.1021/jp030208h CCC: $25.00
Published on Web 07/19/2003

Molecules, AIM), defined by the following simple division rule:

$$\rho_X^{H}(\mathbf{r}) = \rho_X^{0}(\mathbf{r})[\rho(\mathbf{r})/\rho^{0}(\mathbf{r})] \equiv \rho_X^{0}(\mathbf{r})\, W(\mathbf{r}) \equiv \rho(\mathbf{r})\, D_X^{H}(\mathbf{r})$$
$$\rho = \sum_X \rho_X^{H} \quad \sum_X D_X^{H}(\mathbf{r}) = 1 \quad (1)$$

Here $\{\rho_X^0\}$ denotes the densities of the *free* (isolated) *subsystems*, giving rise to the reference electron density $\rho^0 = \sum_X \rho_X^0$ of the isoelectronic "*promolecule*", $\int \rho(\mathbf{r})\, d\mathbf{r} = \int \rho^0(\mathbf{r})\, d\mathbf{r} = N$. It should be observed that the same promolecule reference is used to determine the familiar *density difference function*, $\Delta\rho(\mathbf{r}) = \rho(\mathbf{r}) - \rho^0(\mathbf{r})$, which extracts changes in the electron distribution due to the chemical bonds between subsystems in a molecule. A reference to eq 1 shows that the Hirshfeld densities satisfy the "*stockholder" principle*, that each subsystem participates locally in the molecular "*profit*" $\rho(\mathbf{r})$ in proportion to its share $D_X^H(\mathbf{r})$ in the promolecular "*investment*" $\rho^0(\mathbf{r})$:

$$D_X^{H}(\mathbf{r}) \equiv \rho_X^{H}(\mathbf{r})/\rho(\mathbf{r}) = \rho_X^{0}(\mathbf{r})/\rho^{0}(\mathbf{r}) \equiv D_X^{0}(\mathbf{r}) \quad (2)$$

It also follows from eq 1 that in this partitioning each free subsystem density is locally modified in accordance with the same (subsystem independent) *enhancement factor* as that for a molecule as a whole:

$$W_X^{H}(\mathbf{r}) \equiv \rho_X^{H}(\mathbf{r})/\rho_X^{0}(\mathbf{r}) = \rho(\mathbf{r})/\rho^{0}(\mathbf{r}) \equiv W(\mathbf{r}) \quad X = \mathrm{A, B, ...} \quad (3)$$

Therefore, this common sense local enhancement procedure is devoid of any subsystem bias and appears to be the *objective* one. As indeed demonstrated elsewhere,[1,4,6−9] this division rule has a solid basis in the information theory,[2,3] by minimizing the information distance measure of Kullback and Leibler (cross entropy, directed divergence, missing information, information distance, entropy deficiency) between the AIM pieces of the molecular electron density $\boldsymbol{\rho} = \{\rho_X\}$ and the corresponding free atom densities $\boldsymbol{\rho}^0 = \{\rho_X^0\}$

$$\Delta S[\boldsymbol{\rho}|\boldsymbol{\rho}^0] = \sum_X \int \rho_X(\mathbf{r}) \ln[\rho_X(\mathbf{r})/\rho_X^{0}(\mathbf{r})]\, d\mathbf{r} \equiv \sum_X \int \Delta s_X(\mathbf{r})\, d\mathbf{r} \quad (4)$$

subject to the local constraint of the exhaustive division at each location (see eq 1):

$$\min_{\boldsymbol{\rho}}\{\Delta S[\boldsymbol{\rho}|\boldsymbol{\rho}^0] - \int \lambda(\mathbf{r})\,[\textstyle\sum_X \rho_X(\mathbf{r}) - \rho(\mathbf{r})]\, d\mathbf{r}\} \equiv \sum_X \int \Delta s_X^{H}(\mathbf{r})\, d\mathbf{r} = \Delta S[\boldsymbol{\rho}^H|\boldsymbol{\rho}^0]$$
$$= \int \rho(\mathbf{r}) \ln[\rho(\mathbf{r})/\rho^{0}(\mathbf{r})]\, d\mathbf{r} \equiv \int \Delta s(\mathbf{r})\, d\mathbf{r} = \Delta S[\rho|\rho^0] \quad (5)$$

where $\lambda(\mathbf{r})$ is the relevant Lagrange multiplier function. The stockholder pieces of the molecular electron density exhibit several properties that make them attractive tools for chemical interpretations.[1,4,6−10]

2.2. Displacements of the Molecular Shannon Entropy. In this section we examine the displacements of the overall Shannon entropy[3b,c] of the molecular electron density, $\rho(\mathbf{r}) = Np(\mathbf{r})$, related to the associated probability distribution $p(\mathbf{r})$ (shape function), where N is the overall number of electrons

$$\mathscr{S}[\rho] = -\int \rho(\mathbf{r}) \ln \rho(\mathbf{r})\, d\mathbf{r} \equiv \int \mathscr{s}(\mathbf{r})\, d\mathbf{r}$$
$$= -N\,[\ln N + \int p(\mathbf{r}) \ln p(\mathbf{r})\, d\mathbf{r}] \equiv N\{\mathscr{S}[p] - \ln N\} \quad (6)$$

and of the entropy density $\mathscr{s}(\mathbf{r})$, due to the formation of chemical bonds in the molecule

$$\Delta\mathscr{S}[\rho] = \mathscr{S}[\rho] - \mathscr{S}[\rho^0] \equiv \int \Delta\mathscr{s}(\mathbf{r})\, d\mathbf{r} \quad (7)$$

The density $\Delta\mathscr{s}(\mathbf{r})$ of the entropy displacement functional reflects a local contribution to the overall displacement in the electron uncertainty in the molecule relative to the promolecule. By expressing $\rho(\mathbf{r})$ by $\rho^0(\mathbf{r})$ and $\Delta\rho(\mathbf{r})$ and the first-order expanding the density surprisal,

$$\ln[\rho(\mathbf{r})/\rho^{0}(\mathbf{r})] \cong \Delta\rho(\mathbf{r})/\rho^{0}(\mathbf{r}) \quad (8)$$

$\Delta\mathscr{s}(\mathbf{r})$ can be approximately related to the density difference function:[1,4]

$$\Delta\mathscr{s}(\mathbf{r}) \cong -\Delta\rho(\mathbf{r})[1 + \ln \rho^{0}(\mathbf{r}) + \Delta\rho(\mathbf{r})/\rho^{0}(\mathbf{r})] \quad (9)$$

The entropy displacement of eq 7 can be also expressed in terms of the two directed divergencies[2] (eq 5) of ρ relative to ρ^0 and of ρ^0 relative to ρ, respectively, and the corresponding functional of the density difference function:

$$\Delta\mathscr{S}[\rho] = -\Delta S[\rho|\rho^0] - \int \Delta\rho(\mathbf{r}) \ln \rho^{0}(\mathbf{r})\, d\mathbf{r} = \Delta S[\rho^0|\rho\,] - \int \Delta\rho(\mathbf{r}) \ln \rho(\mathbf{r})\, d\mathbf{r} \quad (10)$$

or

$$\Delta\mathscr{S}[\rho] = 1/2\{\Delta S[\rho^0|\rho] - \Delta S[\rho|\rho^0]\} - \int \Delta\rho(\mathbf{r}) \ln [\rho^{0}(\mathbf{r})\, \rho(\mathbf{r})]^{1/2}\, d\mathbf{r} \quad (11)$$

In the last equation the geometric mean of the two compared electron densities appears, $\rho^g(\mathbf{r}) \equiv [\rho^0(\mathbf{r})\, \rho(\mathbf{r})]^{1/2}$, representing the "*transition" density* between the initial state of the *promolecule* and the final *molecular* state.[6]

The density functional for the Shannon entropy difference can be also related to the corresponding entropy functional of the molecular shape factor ($N = N^0$):

$$\Delta\mathscr{S}[p] = \mathscr{S}[p] - \mathscr{S}[p^0] \equiv \int \Delta\mathscr{s}(p;\mathbf{r})\, d\mathbf{r} = \Delta\mathscr{S}[\rho]/N$$
$$\Delta\mathscr{s}(p;\mathbf{r}) = \Delta\mathscr{s}(\mathbf{r})/N \quad (12)$$

2.3. Entropy Displacements of the Hirshfeld AIM. Similar entropy displacements can be defined for each constituent subsystem, e.g., the stockholder AIM of eq 1:

$$\Delta\mathscr{S}_X^{H}[\rho_X^{H}] = \mathscr{S}[\rho_X^{H}] - \mathscr{S}[\rho_X^{0}] \equiv \int \Delta\mathscr{s}_X^{H}(\mathbf{r})\, d\mathbf{r} \quad X = \mathrm{A, B, ...} \quad (13)$$

Again, by expanding the logarithms of the subsystem surprisals to the first-order, one can approximately relate the integrand of the above atomic entropy difference functional to the Hirshfeld AIM density difference $\Delta\rho_X^H(\mathbf{r}) = \rho_X^H(\mathbf{r}) - \rho_X^0(\mathbf{r}) \equiv N\Delta\rho_X^H(\mathbf{r})$:

$$\Delta\mathscr{s}_X^{H}(\mathbf{r}) \cong -\Delta\rho_X^{H}(\mathbf{r})\,[1 + \ln \rho_X^{0}(\mathbf{r}) + \Delta\rho_X^{H}(\mathbf{r})/\rho_X^{0}(\mathbf{r})] \quad (14)$$

It should be emphasized that the sum of the AIM entropy displacements of eq 13,

$$\sum_X \Delta\mathscr{S}_X^{H}[\rho_X^{H}] \equiv \Delta\mathscr{S}^{a}[\boldsymbol{\rho}^H] = -\sum_X \int \Delta\rho_X^{H}(\mathbf{r}) \ln \rho_X^{0}(\mathbf{r})\, d\mathbf{r} - \Delta S[\rho|\rho^0] \quad (15)$$

defining the *additive* (a) part of the *total* (t) entropy displacement

in the Hirshfeld atomic resolution, $\Delta\mathscr{H}[\rho] = \Delta\mathscr{H}[\sum_X \rho_X^H] \equiv \Delta\mathscr{H}^t[\boldsymbol{\rho}^H]$, differs from the overall entropy displacement $\Delta\mathscr{H}[\rho]$ due to the nonvanishing *nonadditive* (n) contribution:

$$\begin{aligned}\Delta\mathscr{H}^n[\boldsymbol{\rho}^H] &= \Delta\mathscr{H}^t[\boldsymbol{\rho}^H] - \Delta\mathscr{H}^a[\boldsymbol{\rho}^H] \equiv \\ &\sum_X \int \Delta\rho_X^H(\mathbf{r}) \ln \rho_X^0(\mathbf{r})\, d\mathbf{r} - \int \Delta\rho(\mathbf{r}) \ln \rho^0(\mathbf{r})\, d\mathbf{r} \\ &= \sum_X \int \Delta\rho_X^H(\mathbf{r}) \ln D_X^0(\mathbf{r})\, d\mathbf{r} = \\ &\sum_X \int \rho_X^H(\mathbf{r}) \ln \rho_X^H(\mathbf{r})/\rho(\mathbf{r})\, d\mathbf{r} - \\ &\qquad \sum_X \int \rho_X^0(\mathbf{r}) \ln \rho_X^0(\mathbf{r})/\rho^0(\mathbf{r})\, d\mathbf{r} \\ &\equiv \Delta\mathscr{H}[\boldsymbol{\rho}^H|\rho] - \Delta\mathscr{H}[\boldsymbol{\rho}^0|\rho^0] \qquad (16)\end{aligned}$$

In the final part of the preceding equation the nonadditive part of the entropy displacement in the subsystem resolution has been expressed as the difference of two entropy deficiencies between the subsystem densities and the overall density, in the molecule and the promolecule reference, respectively.

The AIM entropy displacements of eq 13 can be also expressed in terms of the corresponding, molecularly normalized shape factors of atomic densities in the molecule

$$\begin{aligned}p_X^H(\mathbf{r}) &= \rho_X^H(\mathbf{r})/N \\ &\sum_X \int p_X^H(\mathbf{r})\, d\mathbf{r} \equiv \sum_X (N_X^H/N) \equiv \sum_X P_X^H = 1 \qquad (17)\end{aligned}$$

and in the isoelectronic promolecule reference:

$$\begin{aligned}p_X^0(\mathbf{r}) &= \rho_X^0(\mathbf{r})/N \\ &\sum_X \int p_X^0(\mathbf{r})\, d\mathbf{r} \equiv \sum_X (N_X^0/N) \equiv \sum_X P_X^0 = 1 \qquad (18)\end{aligned}$$

In eqs 17 and 18 the condensed probabilities in atomic resolution, $\mathbf{P}^H \equiv \{P_X^H\}$ and $\mathbf{P}^0 \equiv \{P_X^0\}$, correspond to events of finding an electron on specific subsystems of the molecular and promolecular systems, respectively. Using the above definitions in eq 13 gives

$$\begin{aligned}\mathscr{H}[\rho_X^H] &= N(\mathscr{H}[p_X^H] - P_X^H \ln N) \\ \mathscr{H}[p_X^H] &= -\int p_X^H(\mathbf{r}) \ln p_X^H(\mathbf{r})\, d\mathbf{r} \\ \mathscr{H}[\rho_X^0] &= N(\mathscr{H}[p_X^0] - P_X^0 \ln N), \\ \mathscr{H}[p_X^0] &= -\int p_X^0(\mathbf{r}) \ln p_X^0(\mathbf{r})\, d\mathbf{r} \qquad (19)\end{aligned}$$

and hence:

$$\begin{aligned}\Delta\mathscr{H}_X^H[\rho_X^H] &= N(\Delta\mathscr{H}_X^H[p_X^H] - \Delta P_X^H \ln N) \\ \Delta\mathscr{H}_X^H[p_X^0] &= \mathscr{H}[p_X^H] - \mathscr{H}[p_X^0] \\ \Delta P_X^H &= P_X^H - P_X^0 \qquad (20)\end{aligned}$$

Therefore, the relation between the entropies of the subsystem electron density and probability distributions, respectively, involves not only the molecule's overall number of electrons, but also a change in the condensed probability of finding an electron on the subsystem under consideration.

3. Numerical Results for Illustrative Diatomic and Linear Triatomic Molecules

The numerical results for selected diatomics and triatomics have been obtained from the DFT calculations using the standard LSDA software (deMon program,[11] DZVP basis set).

3.1. Molecular Displacements. In Figure 1 the $\Delta\mathscr{H}(\mathbf{r})$ plots (second and third columns) are compared with the corresponding density difference diagrams (first column). When interpreting these figures, one should realize that a negative (positive) value of $\Delta\mathscr{H}(\mathbf{r})$ signifies a decrease (increase) of the *uncertainty* of the local electron density in the molecule, relative to the promolecular reference. The $\Delta\rho$ and $\Delta\mathscr{H}$ contour diagrams for the single covalent bond case of H_2 qualitatively resemble one another, with the bonding region exhibiting an increase in the local electron distribution uncertainty. One also detects a similar nodal structure in both maps compared in the figure. The bonding region accumulation of entropy can be attributed to an inflow of electrons in this region and to an extra delocalization of the bonding electrons, now effectively moving in the field of both nuclei. Accordingly, the outer nonbonding regions exhibit a decrease in both the electron density and the associated entropy density. The nonbonding regions thus exhibit a decreased uncertainty, due to an outflow of electrons from this area to the vicinity of the two nuclei and the space between them. The nuclear cusps due to an effective contraction of the AIM electron distributions relative to the free atoms can also be clearly seen in the density difference function diagram. However, the $\Delta\mathscr{H}$ diagram for N_2 is seen to generate a much richer nodal structure in comparison to the corresponding $\Delta\rho$ map. The σ and π electron regions are now found separated by the nodal surface, with additional nodes dividing the inner (in vicinity of the nuclei) and outer (valence) parts of the entropy displacement density. This time, in contrast to the $\Delta\rho$ plot, the molecular entropy difference function reveals a negative feature in the σ component of the triple N≡N bond, thus marking a decrease of uncertainty, relative to the promolecule level, of the σ bond component of the entropy displacement density, in the region around the bond axis. This somewhat unexpected pattern represents the resultant effect of changes in *atomic orbitals* (AO) in the molecule, due to their contraction and hybridization, and due to displacements in their effective occupations, as a result of an effective *excitation* (promotion) of the valence electrons in a molecule. The bonded atoms are promoted to a *"valence state"* configuration, which is effectively excited in comparison to that of the free atoms of the promolecule. This indeed follows from a comparison between the ground-state (valence) electron configuration of the free nitrogen, $N^0 = [2s^2 2p_\sigma^1 2p_x^1 2p_y^1]$, and that characterizing AO of the bonded nitrogen in N_2: $N[N_2] = [2s^{3/2} 2p_\sigma^{3/2} 2p_x^1 2p_y^1]$. The latter directly results from the molecular symmetry and an elementary *molecular orbital* (MO) diagram in the minimum valence basis set, giving rise to the molecular electron configuration, $N_2 = [\sigma^2 \pi_x^2 \pi_y^2 n_1^2 n_2^2]$, where the σ bonding MO represents a symmetric combination of the two (bonding) ($2s$,-$2p_\sigma$)-hybrids directed toward the bonding partner, π_x is the symmetric combination of two $2p_x$ orbitals on both centers, and n_i stands for the nonbonding ($2s_i$,$2p_{i\sigma}$)-hybrid on ith atom directed away from the bonding partner. A reference to both these electron configurations indicates that the bonded nitrogen exhibits an effective $2s \rightarrow 2p_\sigma$ excitation to the amount of half of an electron. This transfer signifies an effective lowering of the symmetry of the atomic σ electrons, in comparison to their state in the promolecule, which implies less uncertainty in their effective distribution in a molecule.

The π bond effect in N_2 involves an increase in the electron uncertainty in the bond region, due to the inflow of electrons from the atomic regions of a maximum electron distribution of the $2p_\pi$ orbitals of the two free nitrogen atoms; indeed, one observes a negative feature in this region, implying a local

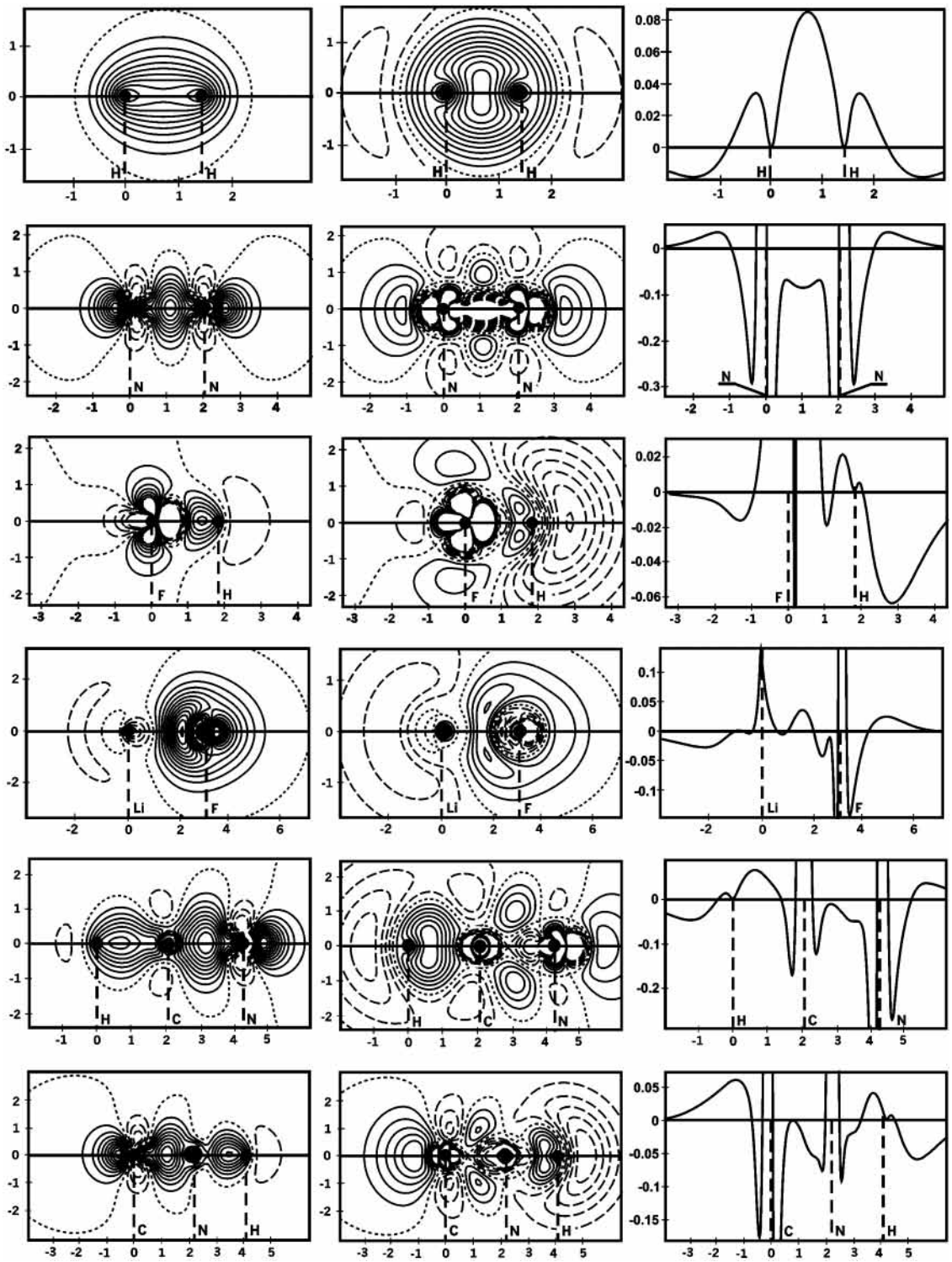

Figure 1. A comparison between contour diagrams of the density difference $\Delta\rho(\mathbf{r})$ (first column) and entropy difference $\Delta\mathcal{H}(\mathbf{r})$ (second column) functions for H_2, N_2, HF, LiF, HCN, and HNC; the corresponding profiles of $\Delta\mathcal{H}(\mathbf{r})$ for the cuts along the bond axis are shown in the third column of the figure. The neighboring contour values are equidistant; the positive (negative) values are represented by the solid (broken) lines, while the dotted line corresponds to the zero value. The same convention is used throughout the paper.

decrease in the entropy difference density. One also detects the buildup of the local uncertainty in the outer regions of the two lone pairs, again a direct manifestation of the $(2s,2p_\sigma)$-hybridization, which accompanies a formation of the σ bond. To summarize, the molecular entropy difference function exhibits explicit manifestations of several familiar stages of the reconstruction of electron distributions in a molecule, relative to those of the corresponding free atoms. As such, the diagrams of this quantity provide a promising new tool for diagnosing the associated displacements in the entropy (information) content of the AIM electron distributions.

Next, let us examine the entropy difference maps for the two heteronuclear diatomics HF and LiF. In HF, the free atoms exhibit lower hardness and electronegativity differences, compared to those in LiF, in which a higher bond ionicity (lower bond covalency) should be expected. The contour maps of the entropy difference functions, again bearing a general resemblance to the corresponding density difference diagrams, reflect

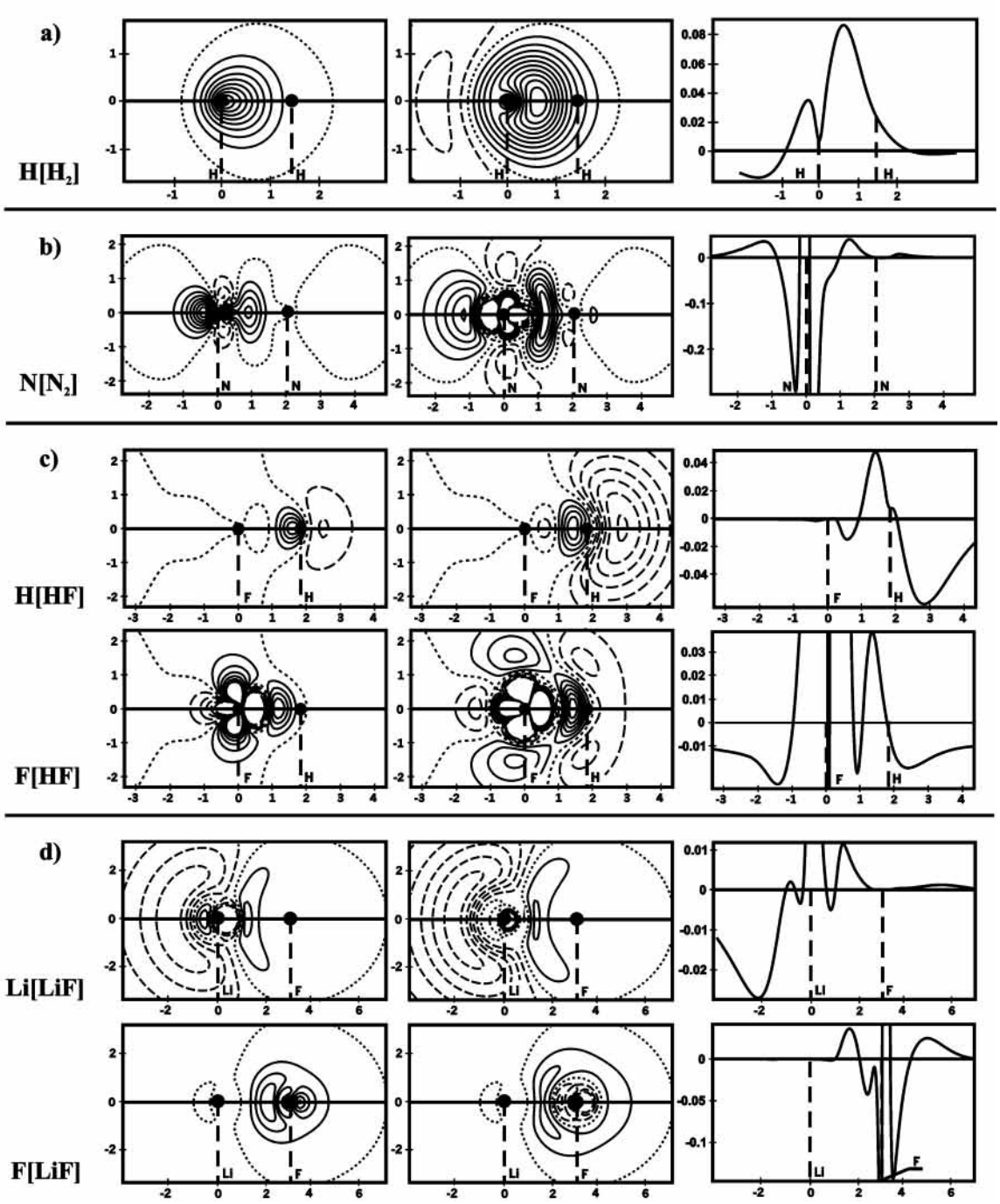

Figure 2. Representative contour maps of $\Delta\rho_X^H(\mathbf{r})$ (first panel), $\Delta\mathscr{S}_X^H(\mathbf{r})$ (second panel), and the $\Delta\mathscr{S}_X^H(\mathbf{r})$ profile of the cut along the bond axis (third panel), for the constituent atoms of diatomic molecules of Figure 1: H_2 (a), N_2 (b), HF (c), and LiF (d).

TABLE 1: Displacements of the Overall Molecular Shannon Entropies for Selected Diatomics and Triatomics

molecule	$\Delta\mathscr{S}[\rho] = N\Delta\mathscr{S}[p]$	$\mathscr{S}[\rho] = N\mathscr{S}[p]$	$\mathscr{S}[\rho^0] = N\mathscr{S}[p^0]$
H_2	−0.84	6.61	7.45
N_2	−0.68	8.95	9.63
HF	−1.00	3.00	4.00
LiF	−3.16	5.12	8.28
HCN	−1.44	12.99	14.45
CNH	−1.39	13.06	14.45

these expected differences in the bond character. In particular, in the HF plot one observes a partial electron transfer from the nonbonding part of the hydrogen distribution to the bonding charge between the two nuclei and to the lone pair AO's on fluorine. An elementary MO diagram involving the valence shell AO suggests that the nonbonding $2p_\pi$ orbital of fluorine, with the occupancy of 5/3 in F^0 and 2 in F[HF], accepts in the molecular valence state 1/3 of an electron each from the σ electrons of both atoms. This $\sigma \rightarrow \pi$ promotion in the molecule is indeed seen in Figure 1. An outflow of the outer part of the hydrogen electron density results in a lowering of the one-electron entropy in that region. A similar trend is detected on Li[LiF], where the inflow of electrons to the fluorine atom results in raising the local entropy values of the outer (valence electrons) above the corresponding F^0 value. Thus, the entropy difference diagrams do indeed appear to be quite useful in monitoring various changes in the electronic structure due to formation of a chemical bond. A comparison between the corresponding HF and LiF contour diagrams clearly indicates

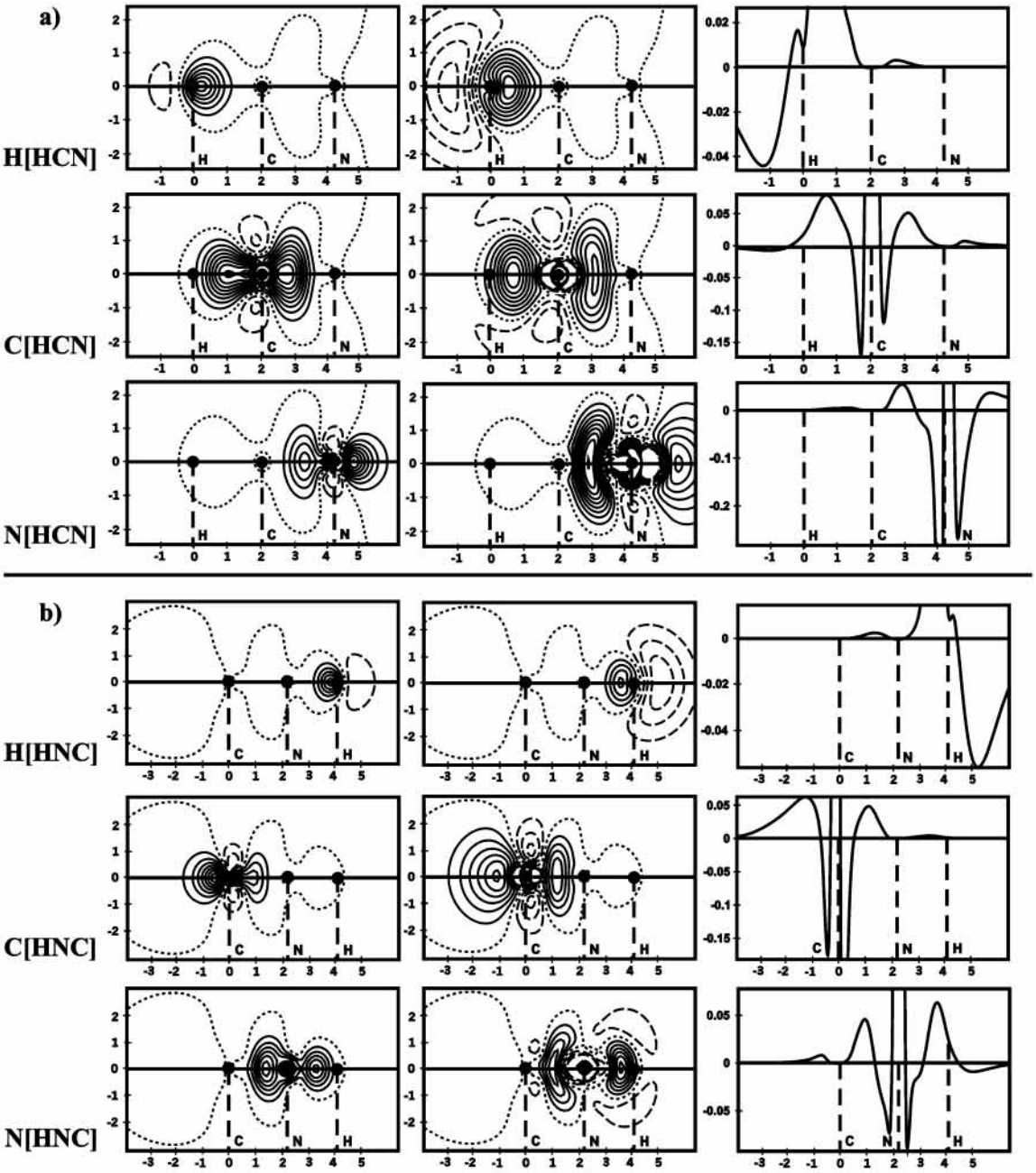

Figure 3. Same as in Figure 2, for HCN (part a) and HNC (part b).

the partial electron-sharing (covalent) character of the bond in HF and the dominating electron-transfer (ionic) character of the bond in LiF.

The remaining two sets of plots in Figure 1 are devoted to the representative linear triatomic isomers: HCN and HNC. In the region of the localized triple C≡N bond, the entropy displacement densities are qualitatively similar to those observed in the N_2, while the mostly covalent C−H and N−H bonds give rise to the entropy displacements strongly reminiscent of those observed in the single H−H and F−H bonds. The effects of the (s,p)-hybridization are again clearly seen on the peripheral heavy atom, and the negative feature of the σ component of the triple bonds is preserved. These results provide an additional confirmation of the applicability of the entropy difference maps in diagnosing the entropy/information origins of chemical bonds.

The plots of Figure 1 demonstrate that the *entropy difference* maps provide a more detailed account of displacements in the electronic structure, relative to that in the free atoms, than the corresponding *density difference* diagrams. In fact, they both constitute tools complementary to the *information distance* probes[1,4] for monitoring changes of the information content displacements of the molecular electron distribution relative to the promolecular reference.

In Table 1 representative integral entropy differences are reported together with the corresponding values of the Shannon entropy for the molecular and promolecular electron densities. These results show that the molecular distributions as a whole are associated with a lower level of the Shannon entropy (less uncertainty, more order) compared to the promolecule reference. When interpreting this general trend, one should realize that there are several aspects of the bond formation that have opposing effects on the overall entropy of the molecular electron distribution. On one hand, a delocalization of electrons through a network of chemical bonds, particularly through their covalent components, increases the degree of uncertainty in the electron distribution. A smaller randomizing effect can be expected from

the charge-transfer, ionic component, since an increase in the entropy of the acceptor atom is then partly canceled by the associated decrease in the entropy of the donor atom. On the other hand, the atomic valence electrons in a molecule are moving in the field of the partially unsreened nuclei of the remaining atoms and thus undergo an effective contraction, which gives rise to more order (less uncertainty) and hence lower entropy in the molecular electron distributions. The results of Table 1 indicate that the latter effect dominates the randomization due to electron delocalization, giving a net negative entropy displacement relative to the promolecular reference.

The largest magnitude is observed for LiF, which exhibits the most ionic bond (highest charge transfer) among all molecules included in the table. There is no obvious correlation, however, between the magnitude of the global entropy displacement and the bond multiplicity, since, for example, a triple covalent bond in N_2 generates less overall entropy loss than a single bond in H_2. Assuming a similar density displacement of about -0.7 for all triple bonds in a series of isoelectronic molecules, N_2, HCN, and CNH, one determines a contribution due to a single C−H or N−H bond of about -0.7, a result close to that obtained for the H−H bond.

3.2. Atomic Displacements. In Figures 2 and 3 we have compared contour maps of the atomic density difference functions $\{\Delta\rho_X^H(\mathbf{r})\}$ of the Hirshfeld AIM with the corresponding entropy difference diagrams $\{\Delta\mathscr{H}_X^H(\mathbf{r})\}$, for the constituent atoms of the representative diatomic (Figure 2) and triatomic (Figure 3) molecules of Figure 1. A reference to the H_2 diagrams (part a of Figure 2) again shows in the density difference plot that the "stockholder" hydrogen H[H_2] does indeed exhibit a charge reconstruction implied by the molecular density difference map of Figure 1. The buildup of the electron density around the nucleus and in the bond region, at the expense of the outer, mainly nonbonding region of the atomic density distribution, is clearly seen in the diagram. This density polarization reflects a contraction of the hydrogen electron density distribution and its expansion toward the bond partner. A similar pattern, be it with a somewhat more emphasized cylindrical polarization toward the other hydrogen, is detected in a qualitatively similar entropy difference plot of the second panel, where the positive part of the AIM entropy displacement, representing an increase in the electron localization uncertainty (delocalization), exhibits a maximum in the bond region. This feature of the atomic local entropy displacement suggests a use of such maps as an alternative tool for monitoring changes in the entropy/information distribution that the bonded atoms undergo in the molecule.

A reference to the N[N_2] plots, shown in part b of Figure 2, further confirms a general similarity between the two types of molecular displacements maps. Shifts observed in the valence shell of both panels accord with the expected valence state changes of the triply bonded nitrogen, mainly due to the $(2s,2p_\sigma)$-hybridization along the molecular axis and a transfer of the $2p_\pi$ electrons to the bond charge region between the nuclei. The entropy displacement map additionally reveals a complicated 1s-core polarization of the bonded nitrogen atoms. Both N[N_2] panels of Figure 2b confirm the molecular character of the Hirshfeld AIM pieces of the electron density, which reflect the whole molecular environment. In particular, the nitrogen displacement "tails" are seen to extend all over the molecule, since each Hirshfeld atom participates in the molecular density everywhere.

Let us now examine the contour maps for the constituent atoms of the two heteronuclear diatomics of Figure 2. In the density and entropy panels for H[HF] (part c), again resembling one another, the hydrogen is seen to be polarized toward the fluorine atom, with the transferred electron density strongly localized in the bond region. This observation supports the conjecture about the strongly covalent character of the H−F bond, compared to that in LiF. The valence-shell, outer part of the F[HF] panels reveals a concerted polarization of the fluorine toward the hydrogen, with the accompanying increase in the lone pair ($2p_\pi$) density, in the direction perpendicular to the bond axis. A complicated displacement in the local information content of the promoted inner electrons is also observed in the right F[HF] entropy density shift panel of Figure 2c. The localization of the fluorine contribution to the bond charge, close to the proton position, also signals the highly covalent character of the chemical bond in HF.

Qualitatively different charge-transfer and entropy displacement patterns are seen for the strongly ionic LiF (Figure 2d). This time both the density and entropy difference diagrams show that the electrons removed from the peripheral part of the electron distribution on Li[LiF] are *transferred* to F[LiF], giving rise to the positive contour values being generally observed *around* the fluorine, with a generally lower degree of localization

TABLE 2: Displacements of the Overall Atomic Shannon Entropies of the Constituent Stockholder AIM in Representative Molecules of Table 1

molecule	AIM, X	$\Delta\mathscr{H}_X^H[\rho_X^H]$	$\mathscr{H}[\rho_X^H]$	$\mathscr{H}[\rho_X^0]$
H_2	H	−0.41	3.77	4.18
N_2	N	−0.34	5.86	6.20
HF	H	−1.09	3.09	4.18
	F	0.03	1.22	1.19
LiF	Li	−4.02	3.87	7.89
	F	0.97	2.14	1.17
HCN	H	−0.87	3.31	4.18
	C	−0.73	7.29	8.03
	N	0.15	6.35	6.20
CNH	C	0.01	8.04	8.03
	N	−0.44	5.76	6.20
	H	−0.98	3.20	4.18

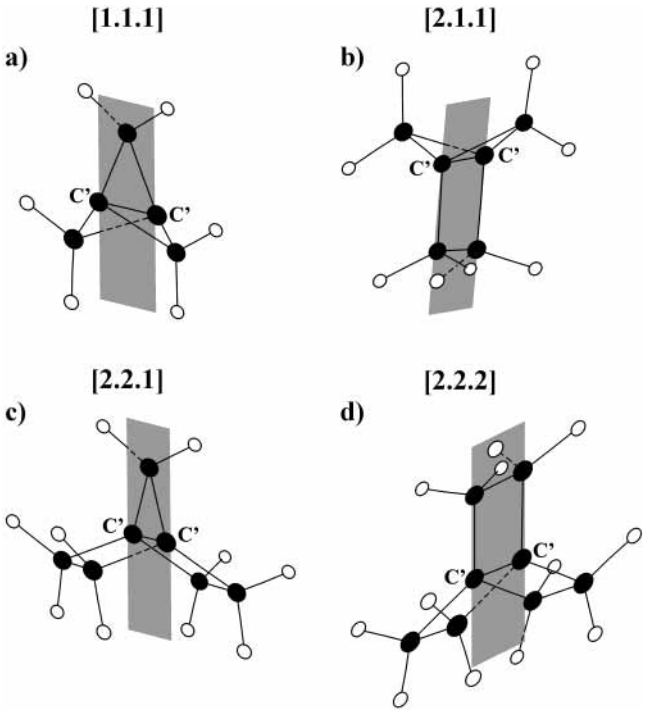

Figure 4. The propellane structures and the planes of sections containing the bridge and bridgehead atoms of the contour diagrams shown in Figures 5 and 7.

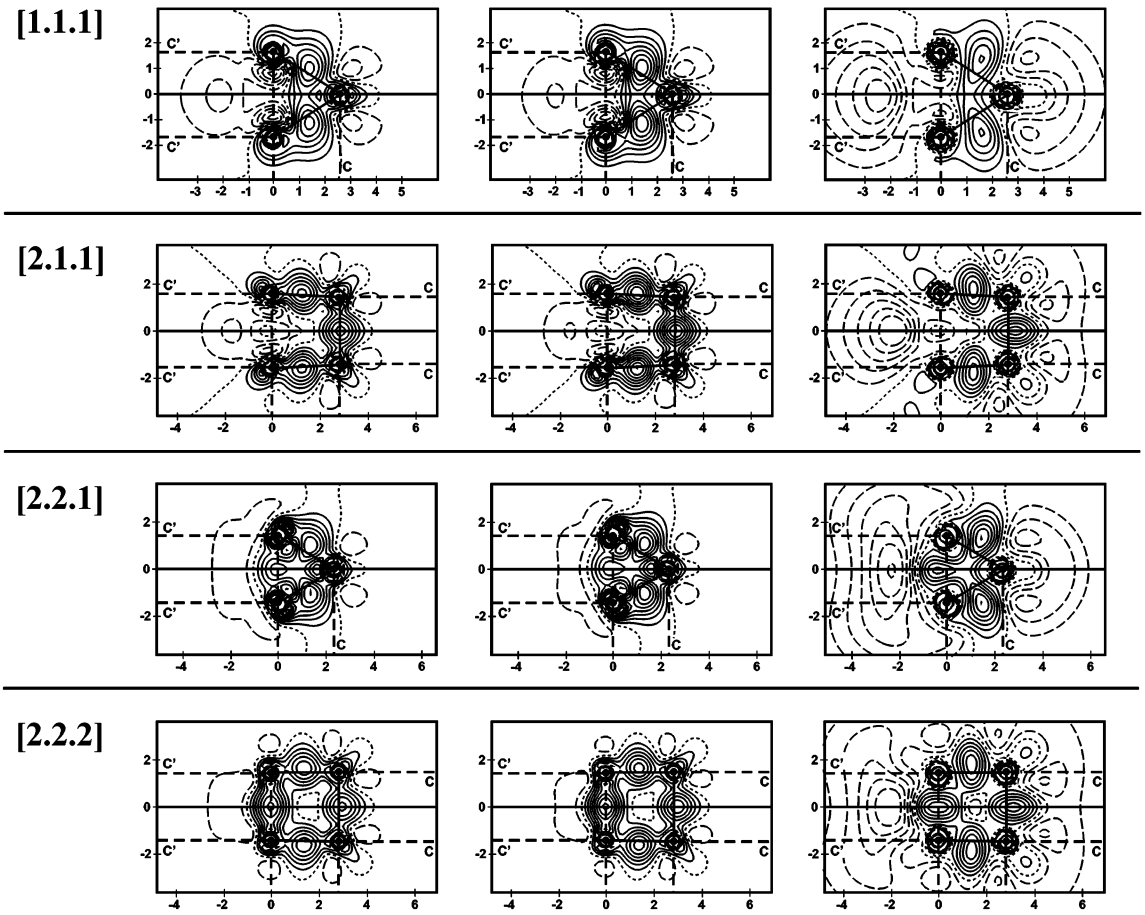

Figure 5. A comparison between the contour maps of the density difference (first column), the information distance density (second column), and the entropy displacement density (third column), for the four propellanes of Figure 4 (see Figure 4 for the definition of the corresponding planes of section).

compared to that in HF. The higher positive contour values on the F[LiF] plots show some concentration of the charge between the nuclei, which implies a partially covalent bond character, much lower though than that observed in HF. The shape of the contours on F[LiF] reveals a low-degree $(2s,2p_\sigma)$-hybridization in valence state.

Finally, we examine the AIM density and entropy displacement plots for the two linear triatomics of Figure 3. All these plots testify to the truly molecular character of the bonded atoms, with the displacements in the atomic electron and entropy densities extending all over the whole molecule. The patterns observed on the corresponding $\Delta\rho_X^H(\mathbf{r})$ and $\Delta\mathscr{S}_X^H(\mathbf{r})$ panels are again qualitatively similar, with the diagrams of the atomic entropy difference additionally separating the outer (valence) and inner (core) effects. The hydrogen maps in both HCN and HNC are seen to involve a density/entropy accumulation in the bond region. The contour diagrams for C and N in both isomers are typical for the valence state displacements on atoms participating in both σ and π interactions with the bond partner again exhibiting the $(2s,2p_\sigma)$-hybridization, a relatively more extended (away from the bond axis) character of the resultant bond charge accumulation due to both σ and π bonds, and the associated removal of electrons from the outer regions of the $2p_\pi$ AO densities.

In Table 2 we have listed representative values of the integral displacement of the Shannon entropy of the Hirshfeld AIM relative to that for the free atom. It should be observed that the compared electron distributions correspond to a slightly different number of electrons, $N_X^H \neq N_X^0$, so that $\Delta P_{Xi}^H \neq 0$ (see eq 20). A reference to the H_2 and N_2 entries of Tables 1 and 2 shows that the atomic displacements are approximately additive: $2\Delta\mathscr{T}_X^H[\rho_X^H] \cong \Delta\mathscr{T}[\rho(X_2)]$. A similar near additivity is observed for the remaining molecules, with the largest deviation being observed for the most ionic bond, Li−F. The atomic entropy displacements for the heteronuclear diatomics indicate that the electron donor atoms, H[HF] and Li[LiF], exhibit a dominating (negative) displacement, while the acceptor, fluorine atom, increases its entropy. The triatomic data of Table 2 provide an additional confirmation of this trend, with the exception of N[CNH]. One detects a relatively strong sensitivity of the atomic entropy displacements to the magnitude of the charge transfer, decreasing with the atomic number of electrons. This should be expected, since a given displacement in the atomic charge in a molecule produces a more dramatic reconstruction of the free atom electron distribution in hydrogen or lithium atoms, compared to that in heavier atoms, e.g., nitrogen or fluorine, as reflected by respective displacements in the atomic shape factors.

4. Central Bonds in Propellanes

The origin of the central bond in propellane systems,[12] between the bridgehead atoms, constitutes a challenging problem for theoretical studies.[13,14] For example, a recent two-electron bond-order study[14] has examined the effect of the bridge size on the overall multiplicity of this bond in the series of [1.1.1]-, [2.1.1]-, [2.2.1]-, and [2.2.2]propellanes (see Figure 4) with increasing bridges. A comparison between the central bond multiplicities, also reported in Figure 6, has shown that an

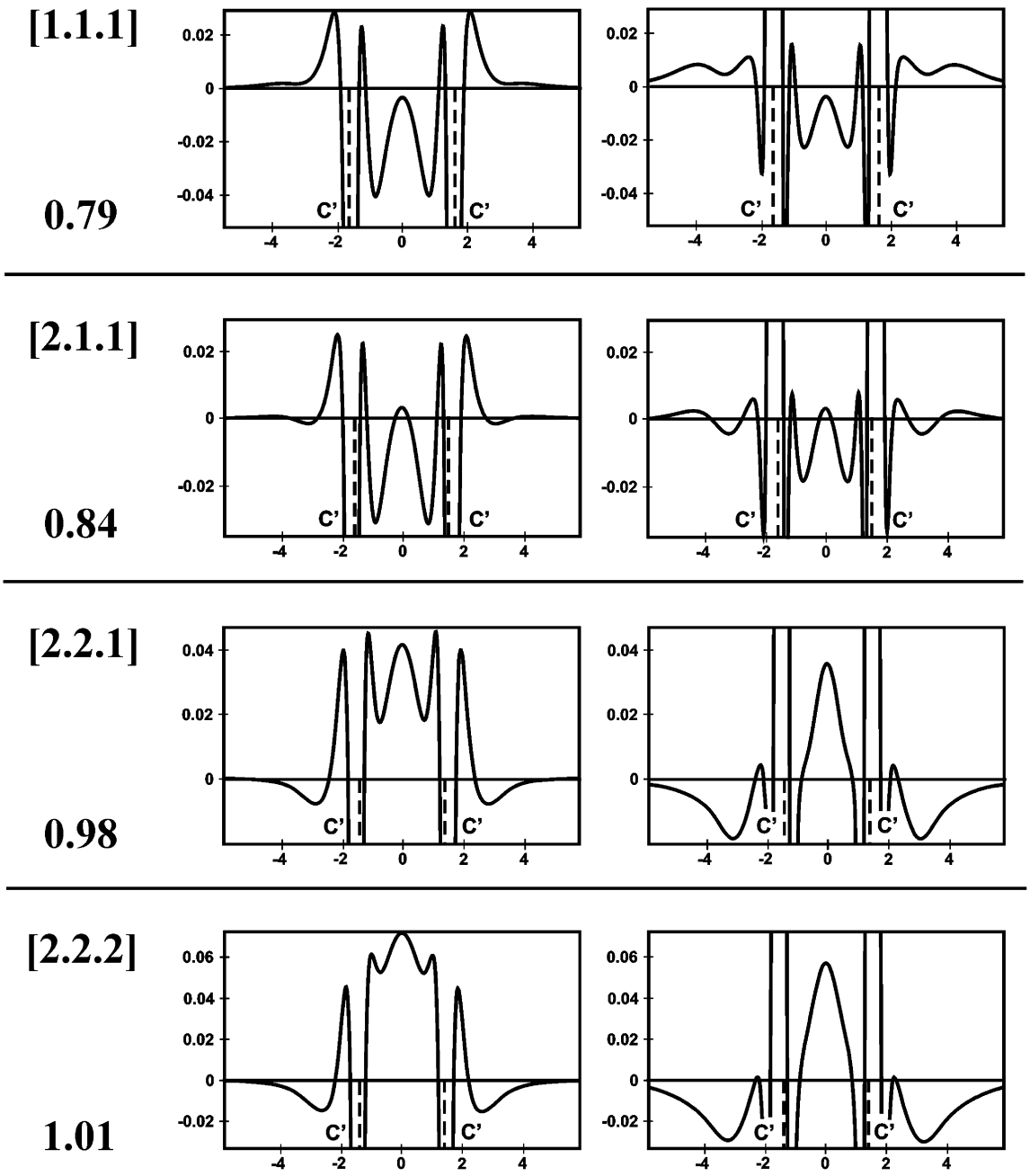

Figure 6. The bridgehead bond profiles of the density difference function (left panel) and molecular entropy displacement (right panel) for the four propellanes of Figure 4. For comparison, the numerical values of the bond multiplicities from the difference approach are reported (from ref 14).

enlargement of the bridge leads to a gradual increase in the magnitude of the bridgehead overall bond order, including the covalent and ionic contributions, from the partial bond of about 0.8 in [1.1.1]propellane to the full bond of multiplicity 1.0 in [2.2.2]propellane. No major changes of the bond orders in the bridges where observed. In this section we examine how does this change in the bond "strength" manifest itself in the corresponding molecular (Figures 5 and 6) and AIM (Figure 7) density/entropy difference diagrams. The corresponding diagrams of the information distance densities $\Delta s(\mathbf{r})$ and their Hirshfeld AIM contributions $\{\Delta s_X^H(\mathbf{r})\}$ of eq 5 are also shown for comparison. The structures and surfaces of sections used in numerical calculations are shown in Figure 4. Both the central and bridge bonds have been examined. In what follows, the primed carbons denote the bridgehead atoms.

The optimized geometries of the propellanes have been determined from the UHF calculations (GAMESS program[15]) using the 3-21G basis set. The remaining molecular properties have been obtained from the DFT calculations using the standard LSDA software (deMon program,[11] DZVP basis set).

4.1. Molecular Displacements. It follows from the density difference maps shown in the first column of Figure 5 and the corresponding profiles of Figure 6 that there is a density depletion between the bridgehead carbons in the [1.1.1]- and [2.1.1]propellanes, while the [2.2.1]- and [2.2.2]propellanes exhibit an electron density buildup in the region of the central bond. The same conclusion follows from examining the information distance maps of the second column in Figure 5. These diagrams are seen to resemble strongly the corresponding density difference plots, since density displacements are relatively small compared to the density itself.[1] One also detects a qualitative similarity between the $\Delta\rho$ (or Δs) contour maps and the corresponding $\Delta\mathscr{H}$ maps shown in the third column of Figure 5 (see also the Δh profiles reported in Figure 6).

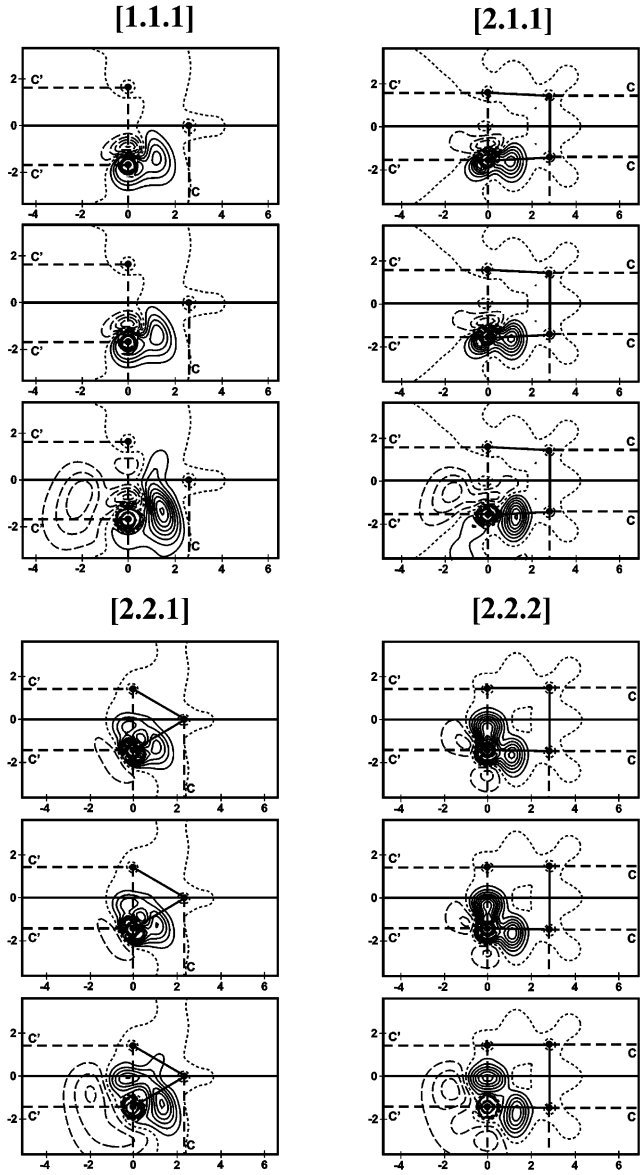

Figure 7. Contour diagrams of the Hirshfeld AIM displacements in the electron density (upper panel), information distance density (medium panel), and the Shannon entropy (lowest panel) for the bridgehead carbon atoms in the four propellanes of Figure 4.

The comparison between the $\Delta\rho$ and $\Delta\mathcal{H}$ profiles and the two-electron bond multiplicities from the difference approach[14] (Figure 6) reveals a changing composition of the central bond in the four propellanes. The smallest bridge case of [1.1.1]-propellane, lacking the bond electron charge accumulation, is mostly "through-bridges" bond in character. A gradual emergence of the "through-space" component, due to a relative increase in the electronic density and the entropy in the central bond region, is observed when the bridges are enlarged. Therefore, one roughly estimates that in the [2.2.1]- and [2.2.2]-propellanes, for which approximately a full single bond is predicted, about 80% is due to the "through-bridge" interactions, a level observed in the smallest [1.1.1]-propellane, and 20% is of the "through-space" origin.

4.2. Atomic Displacements. The Hirshfeld AIM displacement maps of Figure 7, again reporting the related difference functions of the electron density, $\Delta\rho_X^H$, information distance density, Δs_X^H, and entropy density, $\Delta\mathcal{H}_X^H$, support the above conclusions drawn from the molecular data of Figures 5 and 6. The three plots for a given bridgehead carbon atom are seen to be qualitatively similar, thus further validating their possible use as alternative and to a large extent equivalent probes into changes the bonded atoms had undergone in a molecule.

For the [1.1.1]- and [2.1.1]propellanes, lacking the "through-space" component of the central bond between the bridgehead carbons, the buildup in the three densities considered reflects the bridge chemical bonds, with a distinct lowering of the AIM density in the direction of the other bridgehead atom. For the [2.2.1]- and [2.2.2]propellanes, in which the presence of the "through-space" component of the central bond have been inferred from both the molecular density difference and direct bond-order measures, the accumulation of the AIM electron density and the corresponding information distance/entropy densities is observed in the central bond region.

This further confirms a usefulness of the "stockholder" atoms in reflecting the molecular charge and information/entropy displacement distributions. Therefore, they indeed constitute attractive concepts for chemical interpretation of the AIM and origins of the chemical bond in molecular systems.

5. Conclusion

Understanding the origins of chemical bonds is a core issue in theoretical chemistry. The present entropy displacement analysis complements the previous entropy deficiency studies of this problem.[1,4] It further confirms that these information-theoretic quantities can be used as useful diagnostic tools for examining changes in the electronic structure relative to the promolecular reference, before the bond formation. In fact, a general similarity between the contour maps of the electron density difference function and the entropy displacement (or missing information) density indicates that these probes are to a large extent equivalent.[1] This observation allows one to attribute an information-theoretic interpretation to the familiar density difference function. The present analysis of the Hirshfeld AIM displacement quantities gives an additional insight into changes the atoms undergo in the valence (promoted) states in the molecule. These overlapping "stockholder" atoms have been shown to reflect their molecular origin and to exhibit typical changes due to the electron excitation, orbital hybridization, polarization, and charge transfer. As such, they constitute attractive tools for the AIM discretization of molecular electron distributions, i.e., for extracting the chemical interpretation of the calculated electron densities. They are also good candidates for the thermodynamic-like description of molecular systems in atomic resolution.[7−10]

The conditional entropy and information distance concepts have also been used to probe chemical bond multiplicities in model molecular systems[16] using the "communication" system approach to a "transmission" of the AIM assignment information in a molecule. The Kullback−Leibler entropy deficiency has also been used to generate quantitative measures of similarity between the transition-state complex and the reaction reactants/products,[17] complementing the familiar qualitative Hammond postulate[18] or reactivity theory.

Acknowledgment. This work was supported by research grants from the State Committee for Scientific Research in Poland [Grants No. 3T09A 14119 (R.F.N.) and 4T09A18324 (E.B.)].

References and Notes

(1) Nalewajski, R. F.; Świtka, E.; Michalak, A. *Int. J. Quantum Chem.* **2002**, *87*, 198.

(2) Kullback, S.; Leibler, R. A. *Ann. Math. Stat.* **1951**, *22*, 79. Kullback, S. *Information Theory and Statistics*; Wiley: New York, 1959.
(3) (a) Fisher, R. A. *Proc. Cambridge Philos. Soc.* **1925**, *22*, 700. (b) Shannon, C. F. *Bell System Technol. J.* **1948**, *27*, 379, 623. (c) Shannon, C. E.; Weaver, W. *A Mathematical Theory of Communication*; University of Illinois: Urbana, 1949. (d) Abramson, N. *Information Theory and Coding*; McGraw-Hill: New York, 1963. (e) Ash, R. B. *Information Theory*; Interscience: New York, 1965. (f) Pfeifer, P. E. *Concepts of Probability Theory*; Dover: New York, 1978. (g) Frieden, B. R. *Physics from the Fisher Information—A Unification*; Cambridge University Press: Cambridge, 2000.
(4) Nalewajski, R. F.; Świtka, E. *Phys. Chem. Chem. Phys.* **2002**, *4*, 4952.
(5) Hirshfeld, F. L. *Theor. Chim. Acta (Berlin)* **1977**, *44*, 129.
(6) Nalewajski, R. F.; Parr, R. G.*Proc. Natl. Acad. Sci. U.S.A.* **2000**, *97*, 8879.
(7) Nalewajski, R. F.; Parr, R. G.*J. Phys. Chem. A* **2001**, *105*, 7391.
(8) Nalewajski, R. F. (a) *Phys. Chem. Chem. Phys.* **2002**, *4*, 1710. (b) *Int. J. Mol. Sci.* **2002**, *3*, 237. (c) *Adv. Quantum Chem.*, in press; (d) *Chem. Phys. Lett.*, **2003**, *372*, 28.
(9) Nalewajski, R. F.; Loska, R. *Theor. Chem. Acc.* **2001**, *105*, 374.
(10) Nalewajski, R. F. *J. Phys. Chem. A* **2003**, *107*, 3792; *Acta Chim. Phys. Debr.* (R. Gáspár issue) **2002**, *34-35*, 131; *Ann. Phys.*, in press.
(11) St.-Amant, A.; Salahub, D. The LCGTO-LSD-DF program deMon; developed at the University of Montreal, Canada.
(12) Wiberg, K. B.; Walker, F. H. *J. Am. Chem. Soc.* **1982**, *104*, 5239; Wiberg, K. B. *Chem. Rev.* **1989**, *89*, 975.
(13) Jackson, J. E.; Allen, L. C.; *J. Am. Chem. Soc.* **1984**, *106*, 591; Feller, D.; Davidson, E. R. *J. Am. Chem. Soc.* **1987**, *109*, 4133; Wiberg, K. B.; Bader, R. F. W.; Lau, C. D. H. *J. Am. Chem. Soc.* **1987**, *109*, 985, 1001; Bader, R. F. W. *Chem. Rev.* **1991**, *91*, 893; Bader, R. F. W. *Atoms in Molecules: A Quantum Theory*; Clarendon Press: Oxford, 1990.
(14) Nalewajski, R. F.; Mrozek, J.; Mazur, G. *Can. J. Chem.* **1996**, *74*, 1121.
(15) Schmidt, M. W.; Baldridge, K. K.; Boatz, J. A.; Elbert, S. T.; Gordon, M. S.; Jensen, J. J., Koseki, S.; Matsunaga, N.; Nguyen, K. A., Su, S.; Windus, T. L.; Dupuis, M.; Montgomery, J. A. *J. Comput. Chem.* **1993**, *14*, (1347).
(16) Nalewajski, R. F. *J. Phys. Chem. A* **2000**, *104*, 11940; Nalewajski, R. F.; Jug, K. In *Reviews in Modern Quantum Chemistry—A Celebration of the Contributions of Robert G. Parr*; World Scientific: Singapore, 2002; Vol. I, p 148.
(17) Nalewajski, R. F.; Broniatowska, E. *Chem. Phys. Lett.* **2003**, *376*, 33−39.
(18) Hammond, G. S. *J. Am. Chem. Soc.* **1955**, *77*, 334.